Articles

Solid-State Structures of Phenyleneethynylenes: Comparison of Monomers and Polymers

Uwe H. F. Bunz,*,† Volker Enkelmann,‡ Lioba Kloppenburg,† David Jones,† Ken D. Shimizu,† John B. Claridge,† Hans-Conrad zur Loye,† and Günter Lieser‡

Department of Chemistry and Biochemistry, The University of South Carolina, Columbia, South Carolina 29208, and Max-Planck-Institut für Polymerforschung, Ackermannweg 10, 55021 Mainz, FRG

Received January 19, 1999. Revised Manuscript Received March 16, 1999

The solid-state structures of a series of 2,5-dialkyl-substituted poly(*p*-phenyleneethynylene)s (PPEs **4**, R = hexyl, dodecyl, isopentyl, ethylbutyl, ethylhexyl, H) and of 2,5-didodecyl(1,4-phenylenebutadiynylene) were investigated by X-ray powder and electron diffraction. In addition, X-ray single-crystal structures of the monomeric (1,4-dipropynyl-2,5-dialkyl)benzenes were obtained and compared to the structures of the corresponding polymers. In the case of the ethylhexyl-substituted PPE, the packing of the monomer resembles that of the polymer in the solid state. All of the examined PPEs show lamellar morphologies, in which the extended geometry of the side chains determines the value of the lamellar spacing obtained by powder diffraction. A second *d* value, which could be obtained for all samples represents the $\pi-\pi$-stacking distance of the main chains. This distance is around 3.8 Å, a typical value for stacking of aromatic systems. It implies strong electronic interaction of the chromophoric backbones, leading to the observed sharp aggregate band in $CHCl_3$/MeOH solutions and in thin films. From the scattering data, staggered packing of the benzene rings and the phenyleneethynylene main chains in PPEs **4** was inferred. This packing avoids repulsive electrostatic interactions between adjacent conjugated phenyleneethynylene chains and at the same time leads to optimal packing of the side chains.

Introduction

In this contribution the solid-state structures of dialkyl-substituted poly(*p*-phenyleneethynylene)s **4** are investigated. They display highly ordered lamellar phases at ambient temperature, responsible for the occurrence of a well-resolved aggregate band in their solid-state absorption spectra.

Conjugated polymers are organic semiconductors. They have found use as emitting layers in electroluminescent devices and as active media in solid-state "plastic" lasers.[1] The morphology of conjugated polymers is of considerable fundamental interest and important for potential applications[2] insofar as it crucially influences emissive and optical properties. For application in devices, poly(*p*-phenylenevinylene)s, (PPVs, **1**) are

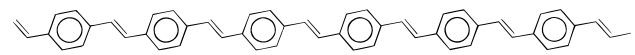

1

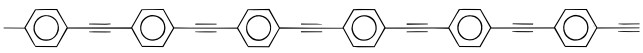

2

well-established, and their physical and structural properties have been extensively studied,[3] including excimer and aggregate formation in solution and in the solid state. Contrary to that, the dehydrogenated congeners of PPV, the poly(*p*-phenyleneethynylene)s (PPEs, **2** and **4**), have attracted much less attention in this regard despite their favorable emission characteristics and high fluorescence quantum yields.[4]

Some structural information upon PPEs has been collected by Weder and Wrighton[5] and more recently by West.[6] However, in both cases *alkoxy*-substituted

* To whom correspondence should be addressed.
† University of South Carolina.
‡ Max-Planck-Institut.

(1) (a) Hide, F.; Diaz-Garcia, M. A.; Schwartz, B. J.; Heeger, A. J. *Acc. Chem. Res.* **1997**, *30*, 430. (b) Pei, Q. B.; Yu, G.; Zhang, C.; Yang, Y.; Heeger, A. J. *Science* **1995**, *269*, 1086. (c) Burroughes, J. H.; Bradley, D. D. C.; Brown, A. R.; Marks, R. N.; Mackay, K.; Friend, R. H.; Burns, P. L.; Holmes, A. B. *Nature* **1990**, *347*, 539. (d) Kraft, A.; Grimsdale, A. C.; Holmes, A. B. *Angew. Chem.* **1998**, *37*, 403.

(2) (a) Neher, D. *Adv. Mater.* **1995**, *7*, 691. (b) Voigt-Martin, I. G.; Simon, P.; Bauer, S.; Ringsdorf, H. *Macromolecules* **1995**, *28*, 236. (c) See also: Rodriguez-Prada, J. M.; Duran, R.; Wegner, G. *Macromolecules* **1989**, *22*, 2507. (d) Müllen, K., Wegner, G., Eds. *Electronic Materials: The Oligomer Approach*; Wiley-VCH: Weinheim, 1998.

(3) (a) Scherf, U. *Topics Curr. Chem.* **1999**, *201*, 163. (b) Conwell, E. *Trends Polym. Sci.* **1997**, *5*, 218. (c) Jenekhe, S. A.; Osaheni, J. A. *Science* **1994**, *265*, 765. (d) Moratti, S. C. In *Handbook of Conducting Polymers*, 2nd ed.; Skotheim, T. A., Elsenbaumer, R. L., Reynolds, J. R., Eds.; Marcel Dekker: New York, 1996.

10.1021/cm990036u CCC: $18.00
Published on Web 04/24/1999

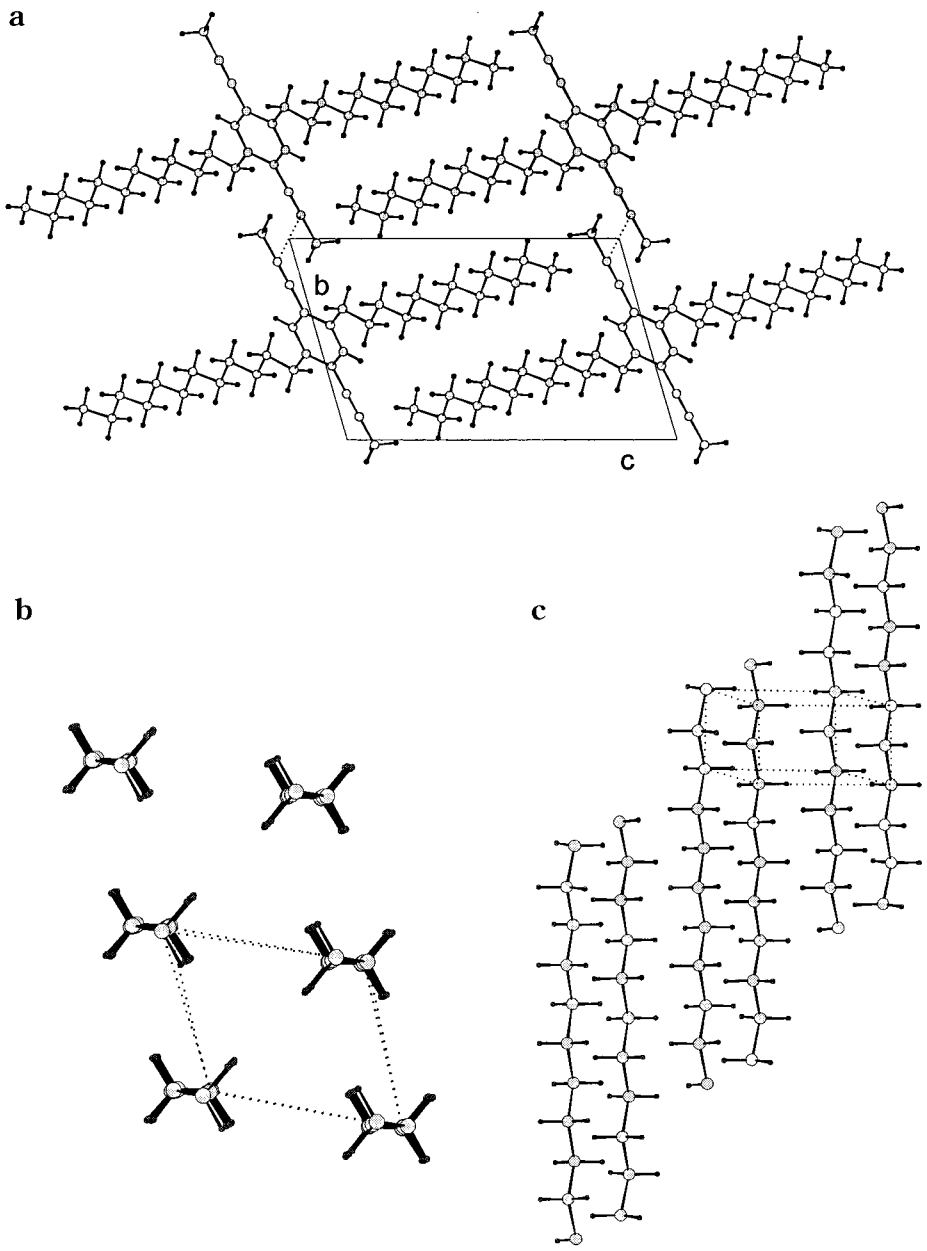

Figure 1. (a) Packing arrangement of **3c** (R = dodecyl); (b) view of the polyethylene subcell in **3c** along the *c* axis (*b* axis in 3*h*−9*h* direction, *a* axis in 6*h*-12*h* direction); and (c) same subcell viewed along the *a* axis (*b* axis in 3*h*−9*h* direction, *c* axis in 6*h*−12*h* direction).

PPEs (**6**) had been examined, and the formation of lamellar or interdigitated phases was suggested.[5] However, no *detailed* picture of their solid state ordering has been offered, and in the case of alkyl-substituted PPEs **4** virtually nothing is known about their morphology.[7]

We have recently found a novel and facile synthetic access to defect-free, high-molecular weight ($P_n \gg 100$), dialkyl-substituted PPEs **4**. We use alkyne metathesis of **3** catalyzed by a mixture of $Mo(CO)_6$ and 4-chlorophenol at elevated temperatures.[8] A series of PPEs has been made and examined in our laboratory with regard to their optical properties. We have found that dialkyl-substituted PPEs (contrary to **6**) form aggregates in the

(4) For high fluorescence quantum yields, see: (a) Mangel, T.; Eberhardt, A.; Scherf, U.; Bunz, U. H. F.; Müllen, K. *Macromol. Rapid Commun.* **1995**, *16*, 571. (b) Davey, A. P.; Elliott, S.; O'Connor, O.; Blau, W. *J. Chem. Soc., Chem. Commun.* **1995**, 1433. (c) Fiesel, R.; Scherf, U. *Macromol. Rapid Commun.* **1998**, *19*, 427. (d) For PPE-based LED's, see: Montali, A.; Smith, P.; Weder, C. *Synth. Met.* **1998**, *97*, 123. (e) For a review about PPEs, see: Giesa, R. *Rev. Macromol. Chem. Phys.* **1996**, *C36*, 631.

(5) (a) Weder, C.; Wrighton, M. S.; Gunter, P. *J. Phys. Chem.* **1996**, *100*, 8931. (b) Weder C.; Wrighton, M. S. *Macromolecules* **1996**, *29*, 5157. (c) Wrighton, M. S.; Ofer, D.; Swager, T. M. *Chem. Mater* **1995**, *7*, 418. (d) Swager, T. M.; Gil, C. J.; Wrighton, M. S. *J. Phys. Chem.* **1995**, *99*, 4886. (e) Steiger, D.; Smith, P.; Weder, C. *Macromol. Rapid Commun.* **1997**, *18*, 643.

(6) (a) Li, H.; Powell, D. R.; Hayashi, R. K.; West R. *Macromolecules* **1998**, *31*, 52. (b) Li, H.; West, R. *Macromolecules* **1998**, *31*, 2866. (c) Li, H.; Powell, D. R.; Firman, T. K.; West, R. *Macromolecules* **1998**, *31*, 1093.

(7) (a) Halkyard, C. E.; Rampey, M. E.; Kloppenburg, L.; Studer-Martinez, S. L.; Bunz, U. H. F. *Macromolecules* **1998**, *31*, 8655. (b) Fiesel, R.; Halkyard, C. E.; Rampey, M. E.; Kloppenburg, L.; Studer-Martinez, S. L.; Scherf, U.; Bunz, U. H. F. *Macromol. Rapid Commun.* **1999**, *20*, 107.

(8) (a) Bunz, U. H. F.; Kloppenburg, L. *Angew. Chem.* **1999**, *38*, 478. (b) Kloppenburg, L.; Song, D.; Bunz, U. H. F. *J. Am. Chem. Soc.* **1998**, *120*, 7973. (c) Kloppenburg, L.; Jones, D.; Bunz, U. H. F. *Macromolecules*, submitted for publication. All monomers and polymers discussed herein are characterized in this forthcoming publication. (d) Weiss, K.; Michel, A.; Auth, E.-M.; Mangel, T.; Bunz, U. H. F.; Müllen, K. *Angew. Chem.* **1997**, *36*, 506.

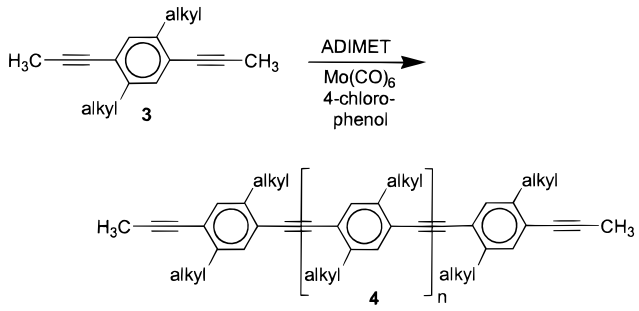

R = **a** Hexyl; **b** nonyl; **c** dodecyl; **d** isopentyl; **e** ethylhexyl; **f** trimethylhexyl; **g** ethylbutyl; **h** (+)-3,7-dimethyloctyl

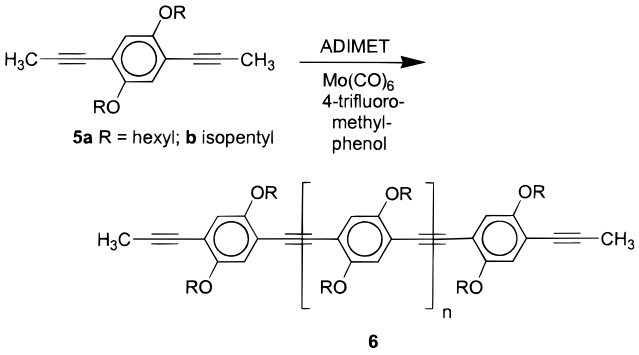

solid state, or upon addition of methanol to their solutions in chloroform. While UV−Vis aggregate bands in polymers are usually broad and unstructured, the newly formed transitions in the absorption spectra of **4** are sharp and well-resolved.[7,9] These species may resemble highly ordered Scheibe-type aggregates, found in low molecular weight merocyanine dyes.[10a,b] Their occurrence in **4** suggested a well-defined and strong interaction of the polarizable π-clouds in the solid state. This made a detailed structural study of dialkyl-disubstituted PPEs necessary with the prospect of unifying spectroscopic and structural data. A combination of different methods, X-ray powder diffraction, electron microscopy, electron diffraction, and molecular modeling was used in this investigation to achieve these goals.

Results and Discussion

Structures and Packing of the Monomers 3 and 5. Single crystals suitable for X-ray structural analysis of the monomers **3a**−**f** and **5a** can be obtained by slow evaporation of their respective solutions in dichloromethane at ambient temperature. Bond lengths and bond angles of **3a**−**f** and **5a** are in excellent agreement with expected values. The packing diagrams of representative examples of the monomers are shown in Figures 1−4 (for cell parameters, see Table 1). With the caveat that a priori prediction of crystal packing is not possible, groups of structurally related compounds offer the opportunity of studying packing arrangements in a systematic way and examining common packing motifs. The derivatives of **3** and **5** present such a case study, with **3a**−**c** and **5a** forming a closely related family. An example of their packing is shown in Figure 1 (**3c**, R = dodecyl) and will be discussed. The solubilizing alkyl substituents are highly ordered (as are all of the *n*-alkyl substituted derivatives, see Supporting Information) and **3c** crystallizes surprisingly well. The side chains of **3c** constitute a major part of the molecule; it is to expect that they influence or even dominate its packing. The dodecyl chains are completely extended and determine the dimension of the *c* axis. They interdigitate to maximize intermolecular *van der Waals* interactions and form a subcell (a = 4.92 Å, b = 4.22 Å, c = 2.53 Å; $\alpha = 89°$, $\beta = 84.5°$, $\gamma = 66.5°$) which corresponds quite nicely to that of triclinic polyethylene (a = 4.82 Å, b = 4.24 Å, c = 2.54 Å; $\alpha = 90°$, $\beta = 80°$, $\gamma = 83°$) as reported by Turner-Jones.[10c]

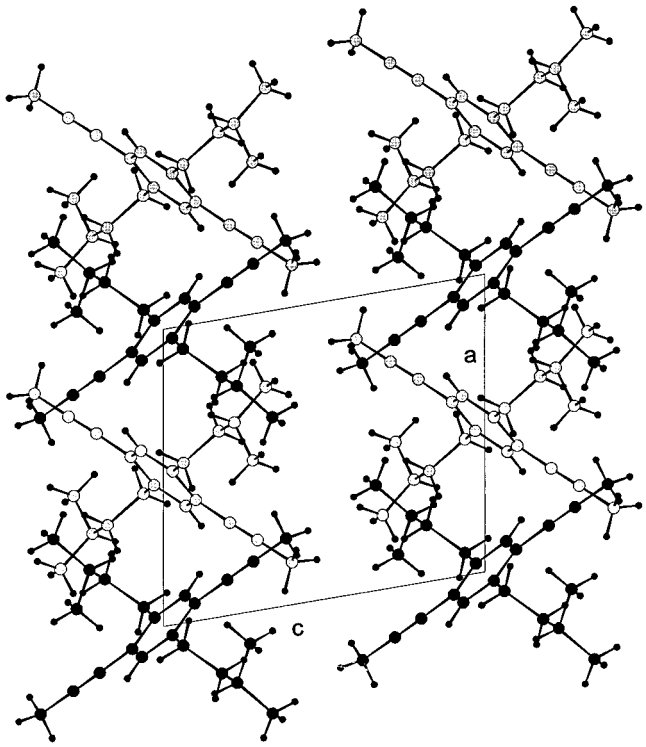

Figure 2. Packing arrangement of **3d** (R = isopentyl).

The lateral distance between two benzene rings is ruled by this packing and can be related to the crystallographic *c* axis (14.3 Å). The *b* axis (9.1 Å) represents the repeating unit along the two 1,4-positioned propynyl groups. This axis equals quite precisely the length of one molecule (~12−2.9 Å) minus the diameter of one methyl group (9.1 Å). In the projection of the structure along the *a* axis, this conforms to the partial overlap of the two propynyl groups in the unit cell. The packing leads to a pattern in two dimensions, which apparently mimics the main chain of the polymer **7a**, with the

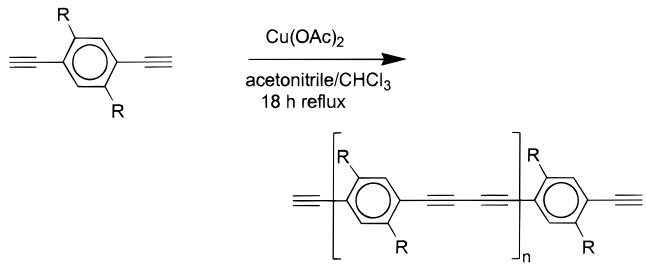

7a, R = dodecyl

(9) Grem, G.; Leising, G. *Synth. Met.* **1993**, *57*, 4105.
(10) (a) Möbius, D. *Adv. Mater.* **1995**, *7*, 437. (b) Scheibe, G. *Angew. Chem.* **1937**, *50*, 51. (c) Turner-Jones, A. *J. Polym. Sci.* **1962**, *62*, 53.

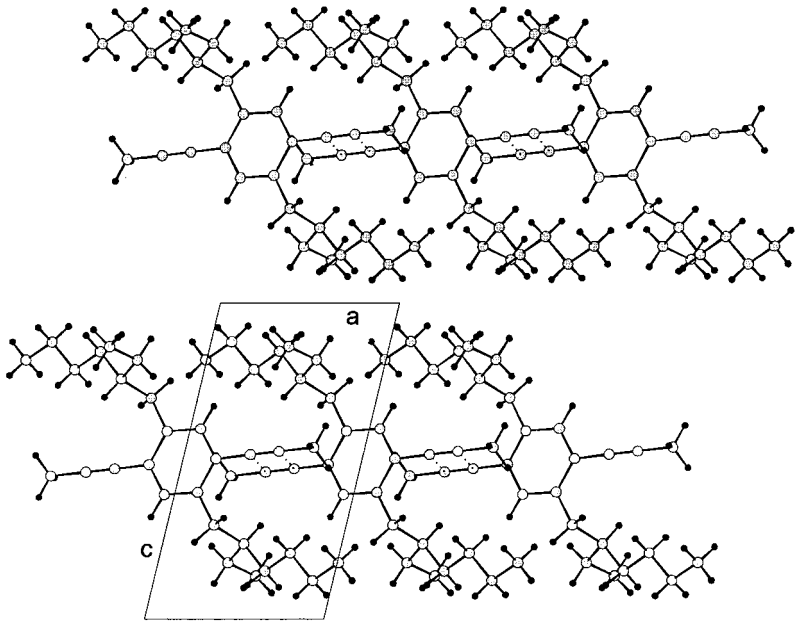

Figure 3. Packing arrangement of **3e** (R = 2-ethylhexyl).

Table 1. Crystal Data for 3a−3f and 5a

	3d	3c	3a	3e	5a	3f	3b
substituent	isopentyl	dodecyl	hexyl	2-ethylhexyl	hexoxy	trimethylhexyl	nonyl
formula	$C_{22}H_{30}$	$C_{36}H_{58}$	$C_{24}H_{34}$	$C_{28}H_{42}$	$C_{24}H_{34}O_2$	$C_{30}H_{46}$	$C_{30}H_{46}$
fw	294.48	490.86	322.54	378.644	354.54	406.70	406.70
space group	$P\bar{1}$	$P\bar{1}$	$P\bar{1}$	$P\bar{1}$	$P\bar{1}$	$P\bar{1}$	$P\bar{1}$
a (Å)	9.514(1)	6.555(1)	6.5993(3)	6.586(1)	6.7585(5)	6.6676(3)	6.7330(3)
b (Å)	10.204(1)	9.071(1)	9.2398(5)	8.391(1)	9.0977(6)	8.2325(3)	9.3043(5)
c (Å)	10.496(1)	14.338(1)	9.9102(4)	12.213(2)	10.034(1)	13.441(1)	11.751(1)
α (deg)	95.663(3)	73.486(3)	64.293(4)	75.71(1)	67.635(7)	76.076(5)	69.24(1)
β (deg)	99.064(3)	85.237(3)	77.095(4)	75.84(1)	72.982(7)	80.788(5)	82.117(4)
γ (deg)	91.233(3)	88.396(3)	87.784(4)	84.78(2)	87.465(6)	80.636(4)	85.316(4)
V (Å^3)	1000.6	814.5	530.0	634.4	544.0	700.9	675.1
Z	4[a]	2	2	2	2	2	2
d (calc) (g cm^{-3})	0.977	1.001	1.010	0.99	1.081	0.963	1.001
μ (cm^{-1})	0.507	0.516	3.850	3.756	4.826	3.642	3.768
total no. of reflns	4120	7941	2775	2406	2205	2841	2802
no. of obs reflns	2117	5338	2021	1753	2004	2278	2205
R (F_o)	0.060	0.082	0.063	0.070	0.071	0.072	0.056
R_w (F_o^2)	0.069	0.089	0.069	0.085	0.078	0.098	0.058
λ	Mo	Mo	Cu	Cu	Cu	Cu	Cu
T (°C)	24	24	24	24	24	24	24

[a] Asymmetric unit consists of two independent half molecules on two centers of symmetry.

numerical value of the *b* axis in **3c** resembling the length of the repeating unit. The two methyl groups in **3c** would fill the space such that they substitute for one alkyne unit in **7a**. The structure of **3c** appears linear and flat only in the projection along the *a* axis. A view along either the *b* or *c* axes shows that the molecules are arranged in steps and do not occur at the same height of the unit cell. The second feature, noticeable in **3c**, concerns the packing of the benzene rings with respect to each other. Molecules **3c** are planar and all of them pack parallel, yet the benzene rings are not positioned on top of each other but the center of one benzene core is located over the propyne unit of the next one. This leads to an offset packing, in agreement with the Seminario−Tour model,[11] satisfying electrostatic demands of the benzene π-faces. Close *inter*molecular contacts (3.71 Å) between two alkyne units of different molecules of **3c** exist, forming an infinite chain. This suggests the possibility of a topochemical polymerization to form a novel polyacetylene derivative. However, irradiation of single crystals of **3c** (λ = 280, 297, 310 nm) with UV light (254 nm) for 16 h neither lead to an appreciable change in color nor to reduced solubility, excluding extensive cross-linking.

Molecules **3f** display a somewhat altered arrangement (Figure 4) when compared to **3c**, the benzene rings in **3f** slightly skipped with respect to the crystallographic *b* axis. The packing of **3d** displays a different motif. The long axes of the two crystallographically independent molecules are arranged in a rhombohedral fashion. They are 45° and 120° tilted in relation to each other (Figure 2). No close intermolecular contacts exist for the C−C triple bonds.

(11) Seminario, J. M.; Zacarias, A. G.; Tour, J. M. *J. Am. Chem. Soc.* **1998**, *120*, 3970.

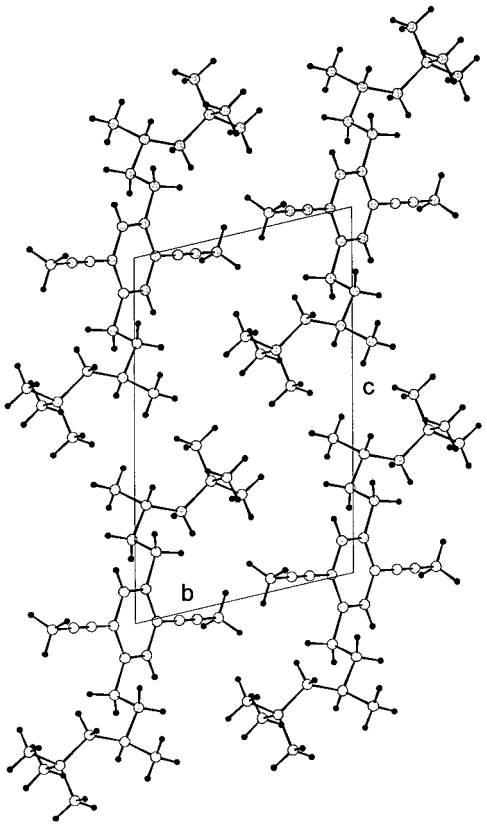

Figure 4. Packing arrangement of **3f** (R = trimethylhexyl).

Of particular interest is the single-crystal structure of the ethylhexyl-substituted monomer **3e**. The packing diagram viewed in the projection of the crystallographic *a* and *c* axes (Figure 3) immediately suggests **3e** as a model for polymer **4e**: The *a* axis (6.59 Å) represents in good approximation the repeating unit of **4e** (6.8 Å) along the conjugated backbone! This is achieved by a step-type packing, in which two of the methyl groups fill the space in the crystal of the monomer **3e**, that otherwise a benzene ring would take up in the polymer.[12] Close interactions (3.83 Å) between the alkyne groups of two molecules of **3e** are observed. This interaction displays polymeric contacts. However, colorless **3e** can be stored for extended periods of time (more than 12 months) in daylight without any visible color change.

In contrast to the other structures (**3a**−**c**, **5a**), the substituents in **3e** are *not* interdigitated, but form lamellae along the *c* axis (12.2 Å). This value corresponds to the lateral extension of the ethylhexyl chains. Monomer **3e** is unique, because it bears two stereocenters each located on one side chain. Our preparation of **3e** is not stereoselective, so a mixture of (*S*,*S*)-**3e**, (*R*,*R*)-**3e**, and (*R*,*S*)-**3e** is expected to form in the process. We performed ^{1}H and ^{13}C NMR spectroscopy on the bulk material but only one signal set was observed for **3e**.[8] However, that does not necessarily imply the stereoselective formation of one single diastereomer. The stereocenters in **3e** are far apart, so that it would not be surprising if the signal sets of different diastereomers were isochronous. We have found similar examples (isochronous signal sets for families of diastereomers) in some organometallic polymers.[13d]

Table 2. Powder Diffraction Data for 2, 4a−f, and 7a[a]

2			5.83, 4.15, 3.89, 3.06
4a	16.23		
4c	25.04	8.49	5.12, 4.58, 4.22, 3.84
4d	13.73	6.82	5.32, 5.08, 4.77, 4.56, 4.36, 3.99, 3.44
4e	12.41	6.10	4.92, 4.26, 4.13, 3.42, 3.08, 2.37, 2.01
4f	17.52	5.69	5.15, 5.00, 4.52, 3.90, 3.71, 3.43
4g	12.58		5.70, 5.04, 4.16
4h	21.25	7.21	
7a	24.92	8.22	

[a] Distances in Ångstroms.

During crystallization of **3e** up to four different types of crystalline species could arise: The *meso*, the (*S*,*S*), the (*R*,*R*), and the conglomerate form. However, in the crystalline specimen examined, only the *meso* (*R*,*S*) form (vide infra) was found.

Polymer Structures in the Solid State. Conjugated rigid rod-type macromolecules can, depending upon their side-chain concentration, display different types of morphologies,[2] including a cylindrical morphology, a lamellar one and an interdigitated packing. The side chains therefore dictate the structure of the polymer to a great extent. In poly(*p*-phenylene)s, the side-chain concentration is high enough to permit a cylindrical arrangement, in which the interaction of the chromophores is greatly decreased, while dialkoxy PPVs typically form lamellae.[2] If the concentration of side chains is reduced further, interdigitated forms such as observed by West et al.[6] prevail. We will show that dialkyl-substituted PPEs are best described as lamellar structures.

Unsubstituted PPE ***2***. The first experiment involved the synthesis of the parent PPE **2**. It was obtained by coupling of 1,4-diiodobenzene to 1,4-diethynylbenzene under standard Heck−Cassar−Sonogashira−Hagihara conditions.[13a−c] A yellow insoluble polymer was obtained in high yield (see Experimental Section). Confirmation of the molecular structure was obtained from CPMAS ^{13}C NMR spectroscopy, which shows only three signals, consistent with the proposed constitution.

The degree of polymerization of this material is low, ∼6−7, due to its insolubility. In the powder diffraction pattern (Table 2) we observe four broad diffraction peaks at 5.83, 4.15 (strong), 3.89 (strong), and 3.06 Å. An X-ray single-crystal structure of the corresponding trimer **8**

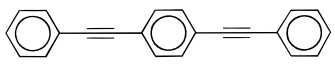

8

has been reported,[6] but the trimers are tilted in the unit cell forming almost s-shaped bands, so that no reasonable conclusion can be drawn from the structure of **8** with regard to the structure of **2**. Likewise it is not trivial to assume a packing pattern. The substituentless rods of **2** can be packed in completely different arrangements, including ones in which the benzene

(12) Eisenbach, C. D.; Nefzger, H.; Hayen, H.; Enkelmann, V. *Macromol. Chem. Phys.* **1994**, *195*, 3325.

(13) (a) Altmann, M.; Bunz, U. H. F. *Angew. Chem.* **1995** *34*, 569. (b) Altmann, M.; Enkelmann, V.; Lieser, G.; Bunz, U. H. F. *Adv. Mater.* **1995**, *7*, 726. (c) Alami, M.; Ferri, F.; Linstrumelle, G. *Tetrahedron Lett.* **1993**, *34*, 6403. (d) Bunz, U. H. F.; Enkelmann, V.; Beer, F. *Organometallics* **1995**, *14*, 2490.

Scheme 1

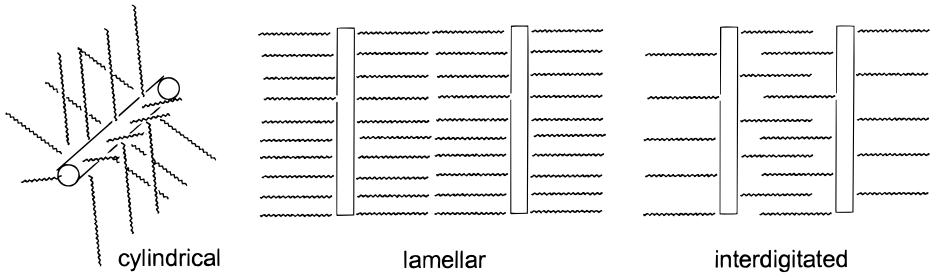

Scheme 2

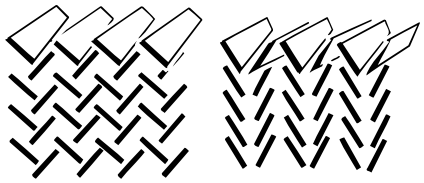

rings are stacked in a herringbone, or a T-shaped/parquet-type motif (Scheme 2). The diffraction data do not allow the formulation of a concise structural model. However, purely parallel packing of the rods in a lamellar fashion is not probable, due to electrostatic reasons that favor edge-to-face packing of the benzene rings. None of the diffraction peaks can be assigned to an intramolecular distance without considerable ambiguity.

*Substituted PPEs **4***. All of the substituted PPEs **4** show similar diffraction patterns although they vary widely in their degree of crystallinity. All of the diffraction patterns contain prominent features due to interlamellar stacking, where the odd order reflections are considerably more intense than the even ones. The same behavior has been observed by Wrighton for alkoxy-substituted PPEs.[5] In the more crystalline samples there are also features present accorded to *intra*lamellar ordering. The diffraction data is summarized in Table 2 and will be briefly discussed on a case-by-case basis.

The diffraction pattern of **4d** (R = isopentyl, and to a lesser extent that of **4g**, R = ethyl butyl) allows us to elaborate a more detailed structural model for dialkyl-substituted PPEs **4**. The prominent feature in the diffraction pattern of **4d** corresponds to a *d* spacing of 13.73 Å. This distance is easily correlated to the end-to-end length in the monomeric unit in which extended isopentyl chains span ~14.8 Å. The side chains are flexible and the 1-Å difference in length can be explained by assuming a slight decrease in the angle between the side chains and the main chain. This includes the concomitant accommodation of the conformation of the isopentyl groups. The observation of the 13.73 Å (001) distance in this polymer supports the formation of a lamellar and not an interdigitated morphology, in which the main diffraction peak would occur at ~7 Å.

The hexyl polymer **4a** reveals only one diffraction peak at 16.23 Å, which we attribute to the lamellar ordering of the side chains. The dodecyl polymer **4c** (see Figure 5a), however, exhibits a more distinct diffraction pattern. The main diffraction peak at 25.04 Å is interpreted as the end-to-end distance between the two dodecyl chains of one ring and constitutes the repeat of the unit cell in one crystallographic direction. In Figure 5b–e the packing of **4c** according to the accumulated data utilizing molecular modeling is displayed. The closest distance between two main chains is 3.8 Å (90° angle). The favorable packing of the side chains dictates this distance, which demands for the main chains to align in register to each other (Figure 5c). This side-chain arrangement reinforces the natural preference of the conjugated backbones to assume a staggered conformation between two chains of the same layer (Figure 5d,e). The lamellar aggregates must display high local order and confer a reasonable degree of crystallinity to the bulk. The linearity of the triple bond is obviously a geometric advantage with respect to the formation of highly ordered lamellae. A diffraction peak at 5.12 Å is interpreted to represent the distance of the main chains observed under an angle of 45°. The increased distance (when compared to the expected distance of 3.8 Å) supports our model that a staggered arrangement of the phenylene units in two adjacent chains of the same lamella occurs. The staggering will increase the periodicity of the diffracting planes to 5.1 Å compared to the distance between the main chains (3.7–3.8 Å).

Decreasing the density of side chains in the polymer should lead to an interdigitated phase. In hope to achieve that, **7a** was synthesized by Vögtle coupling[14] of 2,5-didodecyl-1,4-diethynylbenzene. The P_n of **7a** was ~25, with a polydispersity of M_w/M_n of 7. The polymer is bright yellow and highly soluble in warm chloroform. Powder X-ray diffraction showed *d* values of 24.92 and 8.22 Å. The large *d* spacing however suggests the formation of a lamellar (similar to **4c**) and not an interdigitated phase. The length of the monomer unit in **7a** is ~9.5 Å, apparently not enough to allow interdigitated packing of the dodecyl side chains. A copolymer of the structure **9** with a lower concentration of substituents would probably enforce interdigitation of the alkyl chains.

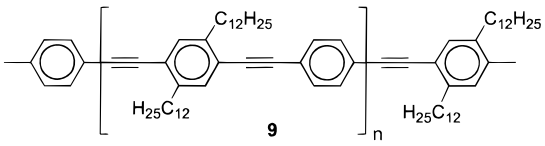

9

*The Ethylhexyl Case **4e***. The most exciting polymer with regard to structure elucidation is **4e**. It is considerably more crystalline than the other examined polymers. Powder diffraction shows prominent *d* spacings at 12.41, 6.10, and 4.13 Å attributable to an interlayer spacing of 12.41 Å, while the peaks at 4.91 and 4.26 Å must be

(14) Berscheid, R.; Vögtle, F. *Synthesis* **1992**, 58.

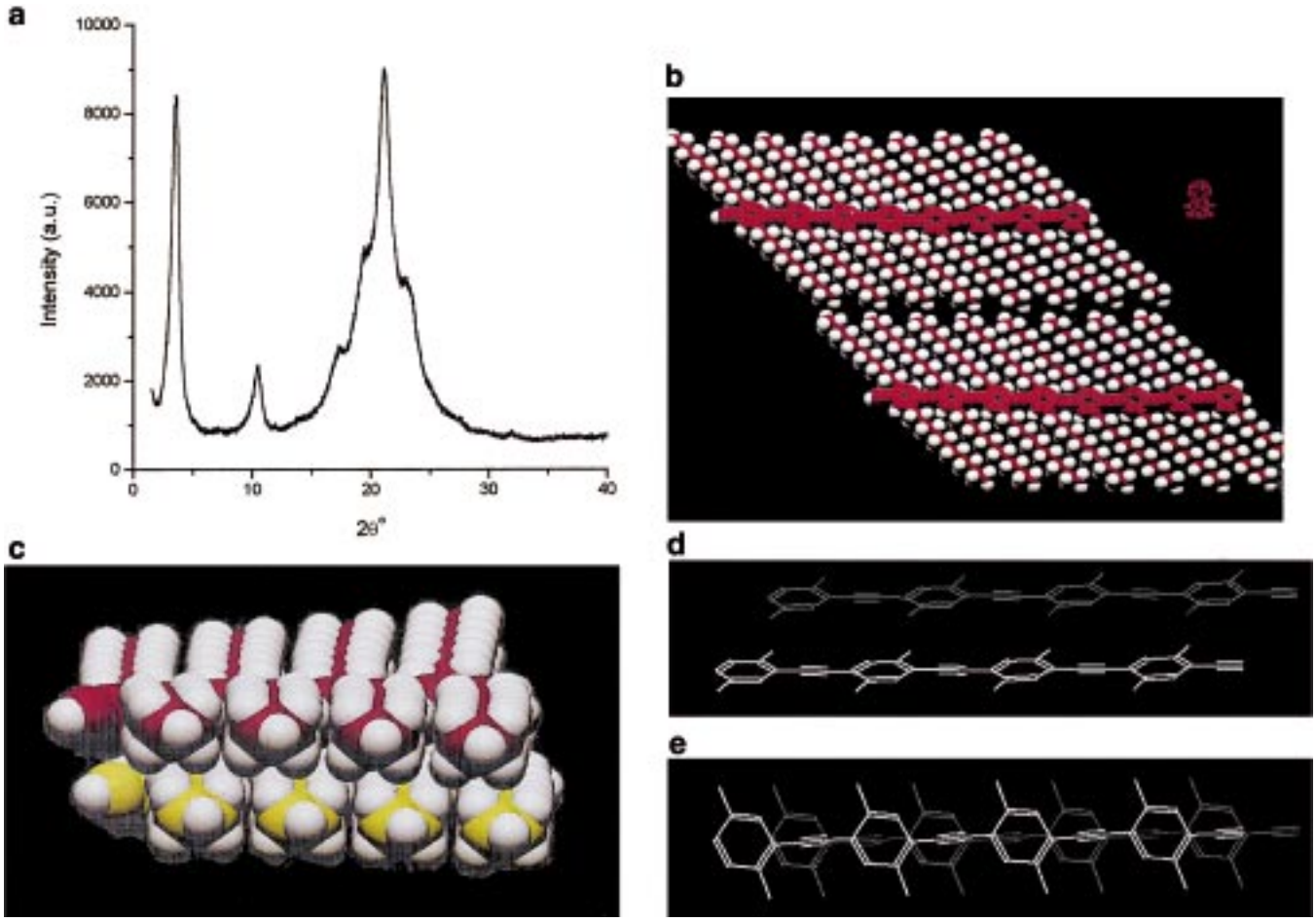

Figure 5. (a) X-ray powder diffraction pattern of **4c**; (b) packing model of **4c** in the solid state (projection along the *c* axis); (c) projection along the *b* axis; (d) side view of the packing arrangement of the main chains (side chains are clipped for clarity); and (e) top view of the packing arrangement of the main chains (side chains are clipped for clarity).

accorded to the arene−arene packing distance. Electron diffraction of a dried oriented lyotropic sample (Figure 6b) does not show the 12.4 Å feature, suggesting that we are looking down the "edge" of the polymer chains. We observe, however, a diffraction peak at 6.8 Å, and one even stronger in intensity at 3.4 Å, which is in excellent agreement with the periodicity expected from one phenyleneethynylene repeating unit along the main polymeric chain. The fact that the second-order reflection (3.4 Å) is considerably stronger than the first-order one corroborates the hypothesis of a staggered packing of the aromatic moieties in the main chains. The crescent assigned to a *d* value of 4.91 Å is the most prominent feature in the electron diffraction pattern. If our picture is correct, benzene rings of two adjacent chains in one lamella should be offset by 3.4 Å, one-half of the repeating unit. If the interchain distance is 3.7−3.8 Å, *the distance between two diffracting planes involving two benzene rings would be in the range of 4.9−5.1 Å in this staggered arrangement*. Additionally, in an ordered sample the crescent (4.9 Å) would not be allowed nor be expected to orient perpendicular to the diffraction features attributed to the intrachain repeating unit in **4e**. Instead the 43° angle between the two diffraction planes in **4e** observed in real space would lead to the loss of a biaxial nature of the diffraction pattern. This is exactly, what we do observe (see Figure 6b).

In Figure 6a, the electron micrograph of **4e** is displayed. It clearly shows a fibrous morphology in which the polymer chains of **4e** must be aligned along the vertical axis of the fibers and the picture. The width of these fibrous features is 36 nm. From the electron diffraction pattern it can be deduced that the observer looks onto the edge of the main chain (vide supra). The rigid polymer chains must be oriented either parallel to the fiber axis (6*h*−12*h* direction) or perpendicular to it (3*h*−9*h* direction), but in any case *in* the plane of the paper. A width of 36 nm would amount to a P_n of ∼50 in **4e**, if the molecules were aligned with their long axis perpendicular to the fibrous structure. This low P_n is in variance with both the NMR and GPC results, which indicate a much higher P_n of 2.0×10^2. Insofar we suggest that the conjugated backbones are oriented in the 6*h*−12*h* direction and form domains in the 9*h*−3*h* direction, which consist of ∼100 main chains stacked on top of each other. The propynyl end groups would be nicely incorporated into these fibrous structures as isomorphous defects, without disrupting the overall crystalline structure.[12]

On another level, we can compare the monomer structure **3e** with that of the polymer. In Figure 7, the simulated powder diffraction pattern of **3e** (from single-crystal data) is overlaid with the actual powder pattern of the polymer **4e**. It is instructive to note that the main diffraction peak in the polymer is located at 12.4 Å,

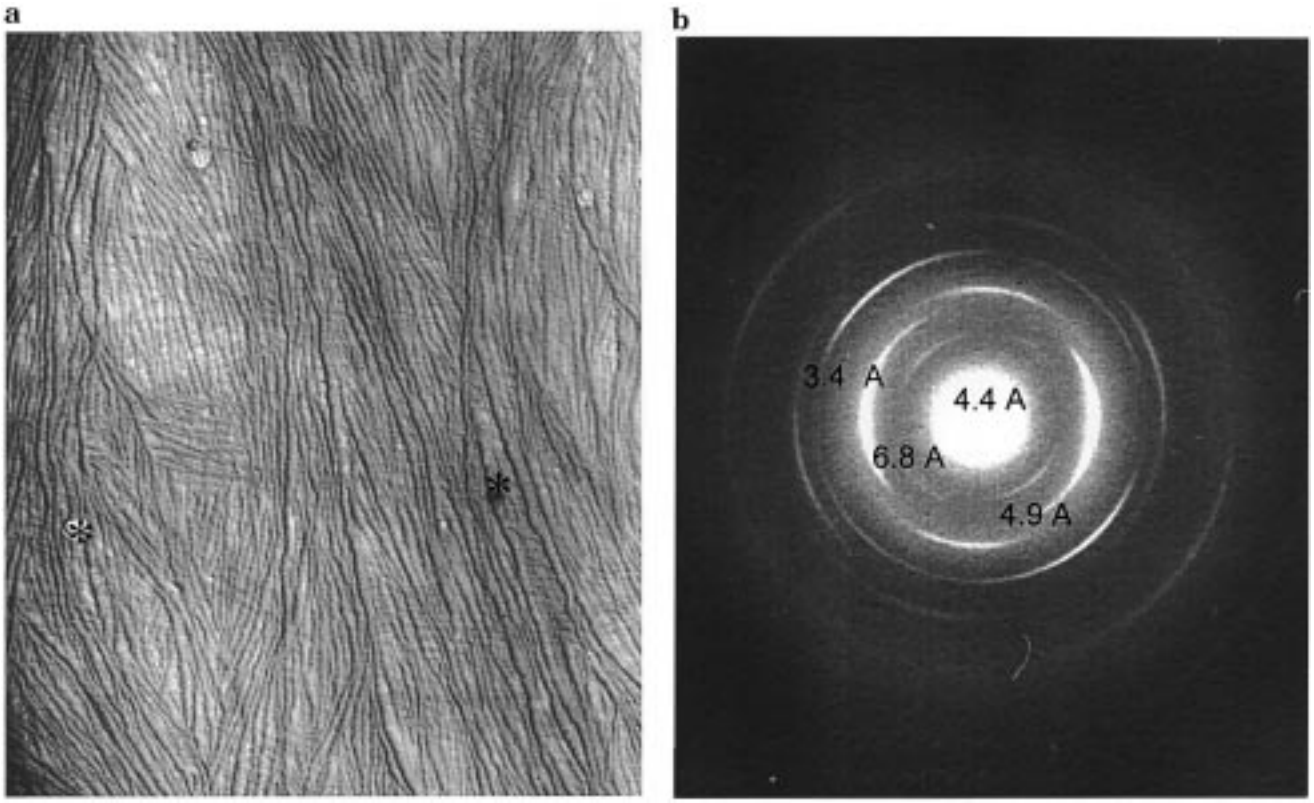

Figure 6. (a) Electron micrograph of **4e** (the two starred features are 2-μm apart) and (b) electron diffraction pattern of a dried lyotropic sample of **4e**.

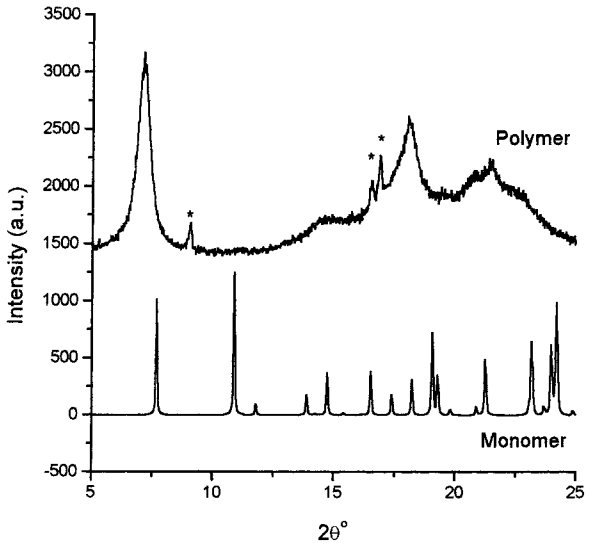

Figure 7. Overlay of the simulated powder diffraction pattern of **3e** with the X-ray powder diffraction pattern of **4e**; * indicates unidentified impurity.

while the analogous *d* spacing of the monomer is only 11.5 Å. Its slightly larger value in the polymer is due to some side-chain crowding, leading to a fuller extension of the ethylhexyl group in **4e** as compared to **3e**. The aromatic stacking distance, in **4e** at 3.7−3.8 Å, is represented in the monomer by the two *d* values of 8.1 and 4.2 Å, respectively. Note, that the phenyl rings are placed directly above each other in every second layer of monomer **3e**. In the alternating layers, two methyl groups of **3e** fill the space, which is taken up by a benzene ring in **4e**. The substitution of one bis(ethylhexyl)benzene unit by two methyl groups renders a surprisingly good, but obviously not perfect model of the polymer **4e**, as can be retrieved from Figure 3.

Conclusions

In this paper we presented the structure of a series of dialkyl-substituted PPEs **4** and their monomers, the dipropynylated benzenes **3**.

- All of the examined PPEs with exception of the unsubstituted polymer **2** form "doubly" lamellar phases or crystallites in which both the side chains and the aromatic moieties of the main chain determine the supramolecular ordering of the polymers. Interdigitated structures are not found, due to the high concentration of side chains in the polymer.
- The parallel packed main chains are at close distance (3.8 Å) and adopt a staggered conformation with respect to each other, i.e., the benzene ring of one polymer chain is located above the alkyne group of the next one with a lateral shift of 3.4−3.5 Å.
- In the case of the ethylhexyl-substituted polymer **4e** the monomer **3e** serves as a reasonable model with respect to the polymer structure, mimicking its lamellar packing.
- A consequence of the strongly interacting π-systems, must be the Scheibe-type aggregate bands in the absorption spectra (annealed films, MeOH/$CHCl_3$ solutions) of **4**.[7] It is however noticeable, that alkoxy-substituted PPEs of similar lamellar solid-state structure do not show such a distinct and narrow aggregate band.

In the future we will deliberately synthesize PPEs in which lamellar packing is prohibited by utilizing *ansa*-substituted and/or more highly branched monomers.

Experimental Section

Instrumentation. Powder diffraction was performed on a Rigaku D/Max 2200 powder X-ray diffractometer at 298 K. Single-crystal structure determinations of **3c** and **3d** were performed on a Nonius Kappa-CCD instrument using graphite-monochromated Mo Kα radiation (see Table 1), while the remaining structures were solved on a Enraf Nonius CAD-4 diffractometer with graphite-monochromated Cu Kα radiation. An empiric absorption correction was applied to the data (Ψ scans). The data collection was in all cases performed at 297 K. The crystal size for **3a**−**f** and **5a** was approximately 0.2 mm × 0.1 mm × 0.4 mm. The structures were solved by direct methods (SIR92), and the non-hydrogen atoms were refined anisotropically. Electron microscopy and diffraction were performed according to the experimental details presented in ref 15. Irradiation of **3c** was conducted for 16 h ($\lambda = 254$ nm) utilizing a hand-held LAMAG UV−low pressure chromatography detection lamp (distance from sample to lamp ∼10 cm). Molecular modeling was performed on a Silicon Graphics O_2 workstation. The calculations were done with MM2 as implemented in MacroModel 5.5.[16] A single polymer chain (octamer) was geometry-optimized and two of these chains were oriented to each other and "bump-check" controlled. No prohibitive van der Waals interactions were observed in the suggested geometry.

Synthesis of 7a. 1,4-Diiodo-2,5-didodecylbenzene (10.0 g, 15.0 mmol), trimethylsilylacetylene (5.00 g, 50.1 mmol), $(PPh_3)_2PdCl_2$ (50.0 mg, 71.2 μmol), and CuI (100 mg, 0.523 mmol) were dissolved in piperidine (50 mL) under an atmosphere of nitrogen. After 3 h, pentane (300 mL) was added and the reaction mixture transferred into a separation funnel and washed with water, dilute ammonia, dilute HCl, and water. Drying over $MgSO_4$ and removal of solvent furnished an off-white solid, which was dissolved in a mixture of methanol (10 mL), THF (10 mL), and dimethoxymethane (10 mL). Concentrated potassium carbonate solution (1.0 mL) was added, and the reaction mixture was stirred for 14 h at ambient temperature. Aqueous workup, double chromatography (silica gel, Merck; hexanes), and crystallization from ethanol furnished 1,4-diethynyl-2,5-didodecylbenzene (4.62 g, 67%) as colorless solid: ^{1}H NMR 7.27 (s, 2 H), 3.26 (s, 2 H), 2.69 (t, 4 H), 1.58 (t, 4 H), 1.24 (s, b, 36 H), 0.86 (t, 6 H); ^{13}C NMR ($CDCl_3$) 143.6, 132.6, 122.0, 82.3, 81.5, 35.3, 33.9, 32.0, 31.4, 30.5, 29.8, 29.7 (2C, overlapped) 29.5, 29.4, 22.7, 14.2.

A round-bottomed flask with a reflux condenser was charged with 1,4-diethynyl-2,5-didodecylbenzene (1.00 g, 2.17 mmol), copper(II) acetate, (5.00 g, 31.7 mmol), acetonitrile (40 mL), chloroform (60 mL), and benzene (20 mL). This mixture was refluxed for 14 h under ambient atmosphere. Addition of dilute ammonia to the reaction mixture and filtration of the formed solid yielded 0.95 g of a tan colored material. Repeated extraction of the raw product with hot chloroform and filtration of the extract furnished **7a** (467 mg 47%) as canary-yellow powder after vacuum-drying: ^{1}H NMR ($CDCl_2$) 7.27 (s, 2 H), 3.26 (s, 2 H), 2.69 (t, 4 H), 1.58 (t, 4 H), 1.24 (s, b, 36 H), 0.86 (t, 6 H); ^{13}C NMR (1,2-dichloroethane-d_4, 95 °C) 143.5, 132.9, 122.1, 82.1, 79.1, 33.8, 31.7, 30.3, 29.5, 29.3, 29.1, 22.5, 13.9; for gel permeation chromatography, polystyrene standard, and conditions see ref 8a,c; $M_n = 11.5 \times 10^3$; $P_n = 25$; $M_w/M_n = 7$; $\lambda_{max} = 411$ nm.

Synthesis of 2. 1,4-Diiodobenzene (2.548 g, 7.72 mmol), 1,4-diethynylbenzene (1.000 g, 7.80 mmol), $(PPh_3)_2PdCl_2$ (30.0 mg, 42.7 μmol), and CuI (100 mg, 0.523 mmol) were dissolved in piperidine (20 mL) under an atmosphere of nitrogen. After 33 h, dilute ammonia was added to the reaction mixture and the suspension centrifuged. Repeated removal of the supernatant, digeration of the yellow residue with first dilute ammonia and then with chloroform followed each time by centrifugation furnished **2** (1.45 g, 92%) as insoluble yellow-ochre powder after drying in high vacuum for 18 h: ^{13}C NMR (CP-MAS) 93.0, 122.8, 132.1.

Acknowledgment. We thank Professor Haskell W. Beckham (Georgia Institute of Technology) for the CPMAS spectrum of **2**. This work was generously supported by the NSF (CHE 9814118; PI Bunz). L.K. thanks the Deutsche Forschungsgemeinschaft, U.H.F.B. is a South Carolina Productive Research Scholar. H.-C.z.L. and J.B.C. acknowledge support by the South Carolina EPSCoR program through NSF/EPSCoR cooperative agreement EPS-9630167.

Supporting Information Available: A listing of atomic coordinates and thermal parameters for **3a**−**f** and **5a** and packing diagrams for **3a**−**f** and **5a**. This material is available free of charge via the Internet at http://pubs.acs.org.

CM990036U

(15) Wang, W.; Lieser, G.; Wegner, G. *Liquid Crystals* **1993**, *15*, 1 and cited references.

(16) Mohamadi, F.; Richards, N. G. J.; Cuida, W. C.; Liskamp, R.; Lipton, M.; Caufield, C.; Chang, G.; Hendrickson, T.; Still, W. C. *J. Comput. Chem.* **1990**, *11*, 440.